Role of void fraction and electrical conductivity in governing microstructural changes and final properties of wheat bread during ohmic baking

Kate Waldert, Sylvie Swyngedau Chevallier, Olivier Rouaud, Alain Le-Bail, Henry Jäger

Applied Food Research 6 (2026) 101824

Contents lists available at ScienceDirect

Applied Food Research

journal homepage: www.elsevier.com/locate/afres

Role of void fraction and electrical conductivity in governing microstructural changes and final properties of wheat bread during ohmic baking

Kate Waldert [a,*], Sylvie Swyngedau Chevallier [b], Olivier Rouaud [b], Alain Le-Bail [b], Henry Jäger [a]

[a] Institute of Food Technology, BOKU University, Muthgasse 18, 1190 Vienna, Austria
[b] Oniris, Nantes Université, CNRS, GEPEA, UMR 6144, F-44000 Nantes, France

ARTICLE INFO

Keywords:
Ohmic heating
Dough properties
Crumb porosity
Bread structure
Microtomography

ABSTRACT

Ohmic baking is a volumetric heating process that exploits the electrical resistance of dough to generate heat, providing a faster and more energy-efficient alternative to conventional baking. To fully harness its potential, a detailed understanding is required of how dough properties affect structural evolution and final bread properties. This study investigated model wheat doughs varying in void fraction (16–69 %) and electrical conductivity (0.4–2.4 mS/cm) to elucidate their influence on process-structure interactions and bread characteristics, including texture, volume, and pore microstructure (via X-ray micro-tomography). Electrical conductivity exerted minimal direct influence on the final bread properties. Nevertheless, higher conductivity levels (>1.0 mS/cm) improved process stability during ohmic baking in the used generator setup by promoting greater current intensity and refined temperature control. Furthermore, void expansion during baking compensated for initial variations in dough conductivity and void fraction, revealing the moderating effects of thermo-electrical interactions on microstructural evolution. Void fraction strongly correlated with final bread characteristics like volume, texture and porosity. Void fractions above 65 % caused excessive pore growth during heating which promoted larger pores and softer crumb, but impaired structure stabilization. Structural fixation occurred near 68 °C, marking the transition between pore expansion and stabilization. The results provide mechanistic insight into the coupled effects of dough properties and electrical behaviour, supporting precise control and tailored application of ohmic baking to produce breads with desired attributes.

1. Introduction

In recent years, ohmic baking has emerged as a fast, energy-efficient alternative to conventional baking. By passing an electrical current through the dough, its intrinsic electrical resistance converts electrical energy into heat, enabling volumetric heating of the product (He & Hoseney, 1991). Unlike traditional oven baking, which is characterized by conventional heat transfer and temperature gradients, ohmic baking delivers energy directly into the product, offering significant advantages in process time, energy efficiency, and costs (Jaeger et al., 2016; Waldert et al., 2025a; Wang et al., 2021). The development of alternative baking technologies is driven by the global energy crisis, sustainability goals, and evolving consumer expectations for high-quality bakery products (Khatir et al., 2013; Le-Bail et al., 2010). Many studies on ohmic baking focused largely on gluten-free breads (Bender et al., 2019; Masure et al., 2019; Pichler et al., 2024; Waziiroh et al., 2023), whereas recent research has increasingly targeted wheat breads due to their high industrial relevance (Derde et al., 2014; Gally et al., 2016; Panirani et al., 2023; Waldert et al., 2025a). For widespread adoption, breads produced by ohmic baking must meet or exceed the quality of conventionally baked products. Achieving this requires a thorough understanding of product–process interactions to design tailored processes that consistently deliver desired outputs.

Electrical conductivity (EC) is widely recognized as the key material parameter governing ohmic heating efficiency and temperature distribution (Jaeger et al., 2016). Previous studies have described changes in EC during ohmic baking as a consequence of physical and biochemical transformations such as volume expansion, water evaporation, and

* Corresponding author.
E-mail address: kate.waldert@boku.ac.at (K. Waldert).

https://doi.org/10.1016/j.afres.2026.101824
Received 14 November 2025; Received in revised form 17 February 2026; Accepted 20 February 2026
Available online 21 February 2026

starch gelatinization (Gally et al., 2016; Kulishov et al., 2020; Waldert et al., 2025b). However, in most cases EC has been treated as a passive system response rather than as an actively adjustable product parameter directly influencing process efficacy.

In breadmaking, salt addition (1–2 %, w/w flour) is known to modify gluten structure, gas retention, and yeast activity (Struyf et al., 2017), while simultaneously increasing ionic concentration and thus EC. Although this dual technological and electrical role of salt is well recognized, the resulting interactions between EC, dough structure, and heating behavior during ohmic baking have not yet been systematically investigated. In contrast, in vegetable and particulate foods, EC-based process control is already well established as a means to effectively regulate and control heating rate and temperature uniformity (Astráin-Redín et al., 2024; Giancaterino & Waldert et al., 2025). The transfer of this concept to dough-based systems remains yet largely unexplored.

Dough microstructure and its evolution during baking play a central role in determining bread volume, crumb texture, and mechanical stability (Jekle & Becker, 2015; Lampignano et al., 2013). While pore formation and structure development during conventional baking of wheat doughs have been extensively studied (Wang et al., 2011), the mechanistic understanding of rapid, volumetric heating processes such as ohmic baking remains limited (Datta et al., 2007). This gap is particularly relevant because ohmically baked breads are typically crustless (Waldert et al., 2025a), eliminating the external mechanical support that normally contributes to structure stabilization. Under these conditions, dough void fraction (DVF) becomes a critical determinant of both heating behavior and structural integrity. Masure et al. (2019) demonstrated that, in gluten-free batter systems subjected to ohmic baking, bread volume and crumb structure are strongly governed by the balance between gas retention and the timing of crumb structure setting. However, gluten-free systems strongly differ from wheat-based doughs and, despite its importance, the dynamic interaction between DVF, EC, and microstructural evolution during ohmic baking of wheat dough has not yet been resolved.

Taken together, existing studies demonstrate that both EC and dough structure strongly influence heating performance, yet their coupled effects in ohmic baking of wheat dough systems remain poorly understood. In particular, there is a lack of systematic studies that simultaneously control dough EC and DVF, monitor their dynamic evolution during ohmic baking, and link these parameters to microstructural development and final bread quality. Addressing this gap is essential for transitioning ohmic baking from a laboratory-scale concept to a robust, industrially relevant process.

Accordingly, this study addressed three main objectives: (i) to establish a reproducible system enabling adjustment of DVF and EC in wheat doughs; (ii) to quantify the influence of initial EC and DVF on heating behaviour during ohmic baking and selected physical bread properties; and (iii) to resolve microstructural development and structure fixation using X-ray microtomography (XMT) at defined baking stages (48 °C, 68 °C, and 98 °C).

2. Materials & methods

2.1. Model dough preparation and determination of void fraction

Two wheat dough recipes were prepared, altering in the addition of salt (sodium chloride). The recipes contained 56.8 % [w/w flour] water, 1.4 % [w/w flour] dry instant yeast (Monoprix Exploitation, Clichy Cedex, France) and either 0.5 % [w/w flour] or 1.5 % [w/w flour] table salt ($K + S$ France SAS, Reims, France), normalized on the content of wheat flour type T.65 (Meunerie Guénégo, Noyal-Muzillac, France).

The model bread doughs were prepared in a standardized procedure using a prototype mixer (VMI, Montaigu Vendée, France), described in detail in Sadot et al. (2017). The mixer features separate controls for the bowl cycloidal movement and the spiral tool orbit, guaranteeing the tool sweeps the entire bowl. The mixing bowl was equipped with a double-jacket circulated by a fluid which temperature can be maintained constant during mixing. It was able to mix bread dough while controlling the headspace pressure (from +500 mbar to −960 mbar gauge pressure). The optimum mixing parameters were determined in pre-trials (data not shown) via determination of the power consumption (Sadot et al., 2017). The mixing time was optimized based on the time needed to reach the maximal value of power consumed by the mixer (time to peak or t_{PEAK}), which is considered as the optimal conditions for dough development. Dough mixing was started with a pre-mixing step for 3 min (100 rpm tool and 8 rpm orbit speed at atmospheric pressure), followed by kneading for 4.5 min (150 rpm tool and 16 rpm orbit speed, 500 mbar gauge pressure with air injection). The dough temperature during kneading did not exceed 25 °C. Dough pieces of desired masses (see below) were weighed and let to rest for 20 min at room temperature under a towel to prevent drying (Jha et al., 2017). Lastly, the dough was shaped using an automatic dough sheeter (L'Artisane 2004, MB 230 Bertrand, Puma – France) before being transferred into the ohmic baking unit, which was placed in the fermentation chamber for proofing (30 °C, 85 % RH).

Altering the proofing time allowed to realize three different initial DVF. Three different proofing times were obtained from three predefined dough volume expansion ratios (Raad et al., 2025). The latter were measured by placing 20 g of dough into a cylindrical sample container (200 ml) and pressing it down to a height of 1 cm, equivalent to zero expansion. Proofing was performed until the dough piece reached 2 cm and 3 cm, corresponding to volume expansion ratios of 2 and 3, respectively. The corresponding proofing times to these expansion ratios were 0 min, 45 min and 90 min, respectively. To further ensure comparable final dough volumes after proofing in the treatment chamber for ohmic baking while still realizing different DVF, different amounts of doughs needed to be used which were 300 g, 450 g and 600 g for proofing times of 90 min, 45 min and 0 min, respectively. This combination of controlled dough expansion and dough mass allowed the ohmic baking process to always start with the same cross-section area of current flow (A) which was essential to differentiate between process- and product-derived effects as the area directly influences the effective conductivity (Eq. (1), Section 2.2). The corresponding DVF after proofing was determined at least in triplicates via Archimede's principle following the method described by Sadot et al. (2017). For doughs, the term DVF (ε_{Dough}) is used whereas for bread, the term porosity (ϕ_{Bread}), will be introduced (see Section 2.3).

2.2. Ohmic baking and determination of electrical conductivity

A prototype ohmic heating unit with stainless steel electrodes (initial dimensions of 27.5 cm x 10 cm (L x H), thickness of 2 mm) in parallel-plate configuration was used for baking, described and visualized in detail in Gally et al. (2017), with some slight modifications. Briefly, the baking chamber volume was reduced to allow baking of dough pieces of up to 600 g by reducing the distance between insulators. In this way, the electrode thickness of 2 mm and distance of 10 cm was kept identical but the electrical resistance of the chamber was reduced to meet the current limit of 3 A of the prototype system. The modified treatment chamber dimensions were 15 × 10 × 10 cm (L x W x H), where the effective initial electrode area of current flow was 15 × 5 cm (L x H) for all experiments, as visualized in Fig. 1.

The process set-up was developed in pre-trials by testing different voltages (120–220 V) resulting in different heating rates of 6–30 °C/s (data not shown) targeting a high heating rate and the voltage was adapted accordingly within the technical feasibility of the generator (max. current flow of $I = 3$ A). The heating rate was controlled using a human machine interface and programmable logic controller (Unitronics Vision 700) and proportional–integral–derivative controller (variable transformer 240 V and 720 VA, RS-Pro 890–2777 and solid state relay CRYDOM CKRD2410). The dough was heated until reaching

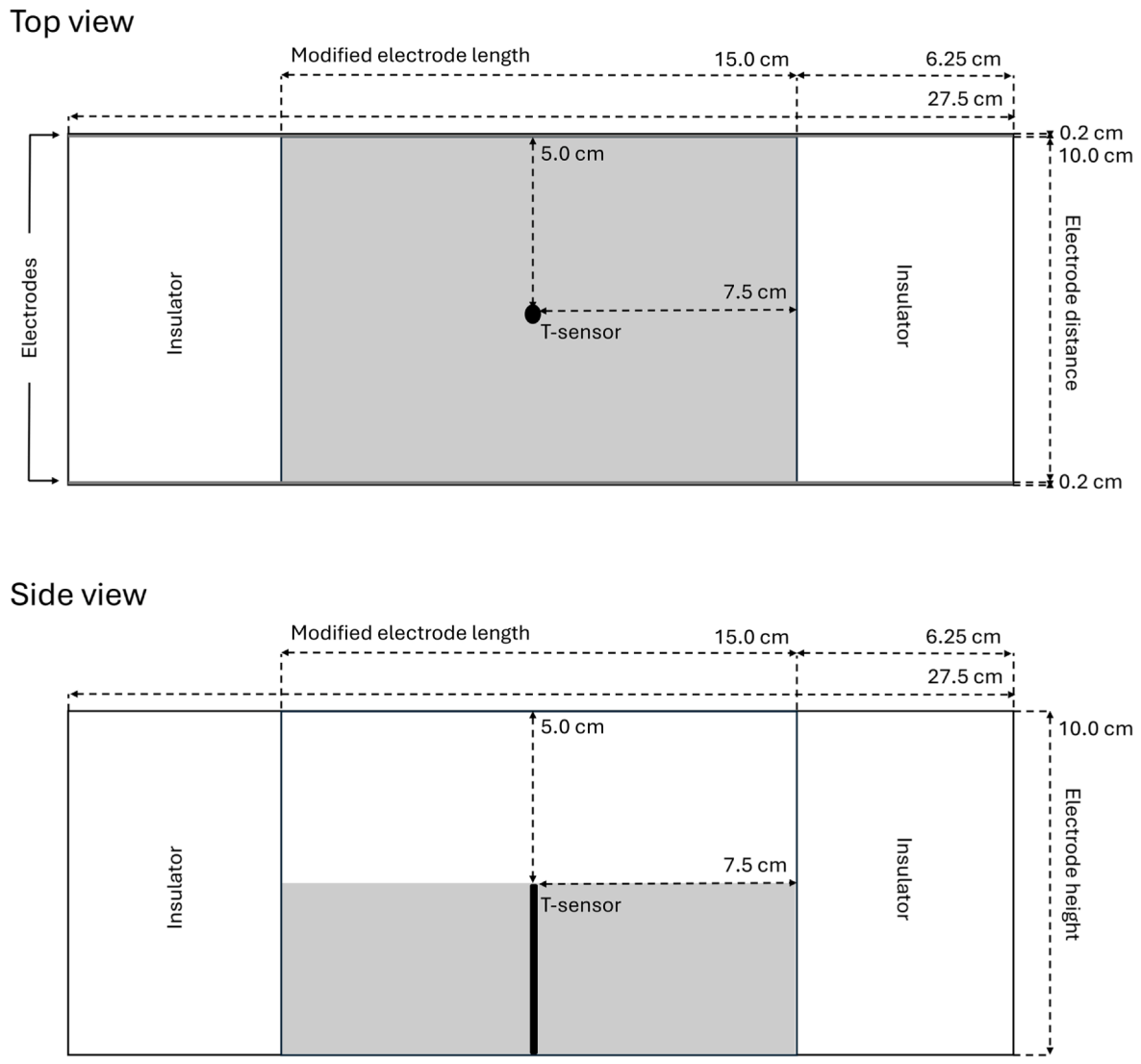

Fig. 1. Schematic of top and side view of the treatment chamber used for ohmic baking including dimensions of important chamber parts. The effective initial electrode area of current flow (covered by dough in the beginning of the baking process) is highlighted as grey area. The thermocouple (T-sensor) in the geometrical center of the treatment chamber is shown in black.

a plateau value of 98 °C (measured in the geometrical center of the modified treatment chamber at a fixed height of $h = 5$ cm by a mineral insulated thermocouple K-type) within 12 min using a constant AC electric field strength of 15 V/cm ($U = 150$ V, $f = 50$ Hz), followed by a holding phase for 3 min at same conditions. The current intensity [A], voltage intensity [V] and power input [W] were monitored internally during processing. The total energy consumption [MJ/kg] of each baking process was calculated as the sum of the accumulated power input of all pulses [MJ] divided by the dough mass [kg]. The heating rate [K/min] was quantified via linear regression ($R^2 \geq 0.997$) for the linear part of temperature increase (30–70 °C). The EC (σ) was calculated for dough and bread according to Eq. (1) (Waldert et al., 2025b).

$$\sigma = \frac{U \cdot L}{I \cdot A} \quad (1)$$

Here, U is the applied voltage [V], L is the electrode distance [L], I is the applied current [A] and A is the area of current flow [m^2]. Although the progression of EC during ohmic baking would have given valuable insights into the product-process interactions, the modified ohmic equipment did no longer allow the in-line laser measurement of dough height. The EC of the dough was calculated with the initial current intensity and dough height ($h = 5$ cm) for the determination of the area of current flow. For the EC of the breads, final average heights of breads in the end of baking were used for calculations of A (see Table 1).

Intermediate baking steps were investigated for doughs featuring 0 min and 90 min proofing time to evaluate microstructural changes at critical stages during the baking process. The process was stopped when the dough reached core temperatures of 48 °C, 68 °C and 98 °C, respectively, representing temperatures below (48 °C), around (68 °C) and above (98 °C) the gelatinization temperature of wheat starch (Li et al., 2004), hypothesized to directly influence structure fixation. After baking, all samples were cooled down to room temperature (20 ± 2.0 °C) within 2 h before further analysis. Baking trials were performed in triplicates, except for analysis of intermediate baking steps where duplicates were performed.

2.3. Physical bread characterization

Physical bread characterization was carried out in triplicates, using three individual loaves per condition. Baking loss was determined gravimetrically as the ratio of dough weight to loaf weight after 2 h of cooling. Loaf volume was measured with a bread volume analyzer (TexVol BVM-L37 OLC, Perkin Elmer, Waltham, MA, USA), and specific volume was calculated as the ratio of loaf volume to loaf weight. To

Table 1
Dough void fraction (ε)/ porosity (ϕ) and electrical conductivity (σ) of model doughs and corresponding breads as well as power consumption during the ohmic baking process.

Dough	Salt content [% w/w flour]	Proofing time [min]	m_{Dough} [g]	ε_{Dough} [%]	σ_{Dough} [mS/cm]	ϕ_{Bread} [%]	σ_{Bread} [mS/cm]	h_{Bread}* [cm]	Power consumption [MJ/kg]
A	**0.5**	**0**	300	19.8 ± 1.2^{B}	0.9 ± 0.1^{C}	69.8 ± 2.7^{B}	0.8 ± 0.1^{B}	7.7	0.31 ± 0.01^{AB}
B		**45**	450	54.5 ± 4.1^{D}	0.7 ± 0.1^{B}	77.5 ± 1.4^{C}	0.6 ± 0.1^{B}	9.3	0.31 ± 0.01^{AB}
C		**90**	600	65.3 ± 3.5^{E}	0.4 ± 0.1^{A}	81.8 ± 0.7^{D}	0.3 ± 0.1^{A}	9.6	0.30 ± 0.01^{A}
D	**1.5**	**0**	300	15.9 ± 2.1^{A}	2.4 ± 0.2^{E}	65.9 ± 2.3^{A}	2.2 ± 0.2^{D}	7.6	0.31 ± 0.02^{AB}
E		**45**	450	44.2 ± 2.4^{C}	1.4 ± 0.2^{D}	74.6 ± 0.9^{C}	1.4 ± 0.1^{C}	8.4	0.33 ± 0.03^{B}
F		**90**	600	68.7 ± 1.7^{F}	1.0 ± 0.1^{C}	81.9 ± 0.4^{D}	0.7 ± 0.1^{B}	8.7	0.43 ± 0.02^{C}

Dough properties refer to the start (25 °C) and bread properties to the end of ohmic baking (98 °C) with values reported as technical replicates ($n = 3$). Significant differences ($p < 0.05$) are marked as different capital letters within one data column.
* The initial height for all doughs was 5 cm.

evaluate the bread porosity (ϕ_{Bread}), Eq. (2) was used (Varayil et al., 2019).

$$\phi_{Bread} = 1 - \frac{\rho_{app}}{\rho_{true}} \quad (2)$$

Here, ρ_{app} is the apparent density of the bread, calculated as reciprocal of its specific volume, and ρ_{true} is the true density, measured with a helium pycnometer (AccuPyc 1330, Micromeritics GmbH, Unterschleißheim, Germany). For two-dimensional (2D) crumb structure analysis, loaves were sliced into 1.3 cm slices using an automatic slicer. Slice scans were acquired (V600 Photo, Seiko Epson Corporation, Suwa, Japan), and image analysis was performed in ImageJ (version 1.54d, NIH, Bethesda, USA) following Waldert et al. (2025a). The evaluated parameters included average pore size, pore count, and pore inhomogeneity, reported per analyzed area (20 × 20 mm). Crumb texture was assessed with a texture analyzer (TA1, AMETEK Inc., Berwyn, USA) equipped with a 50 N load cell. A 2.5 cm cylindrical probe performed a 50 % single compression test at the geometric center of each bread slice, followed by a 120 s holding phase (Pichler et al., 2024). Crumb hardness was defined as the peak force [N] at 50 % compression, while relative elasticity [%] was calculated as the ratio of force at 120 s to peak force (Rumler et al., 2023). Three slices per loaf were analyzed, equal to nine slices per recipe and proofing time.

2.4. Analysis of microstructure

The microstructure of samples was observed and analyzed by XMT, a non-destructive technique which obtains a three-dimensional (3D) representation of the internal sample structure (Chevallier et al., 2014). All samples of dough were quickly frozen in cylindrical sample containers after proofing (as explained in Section 2.1) by placing them in a Dewar containing solid CO_2 and then stored in a freezer at −40 °C. Bread samples were sliced before freezing (see Section 2.3). Partially baked doughs cooled down before samples were cut manually from the geometrical center and frozen in cylindrical sample containers. Preliminary tests (data not shown) were performed to measure the temperature inside frozen dough samples during XMT acquisitions and define XMT acquisition parameters preventing samples to defreeze. They were set up at 70 kV, 500 µA, exposure time 500 ms, and 960 projections were acquired on a 360° rotation.

Data acquisition was performed with an EasyTom 150 (RX Solutions, Chavanod, France) equipped with a 150 kV sealed tube generator and a flat panel (2560 × 2048 pixels). A voxel size of 50 × 50 × 50 μm^3 was chosen for all the acquisitions as the best compromise between sample size, resolution and computation time for the image analyses. Volume data were reconstructed using the filtered back projection algorithm of X-Act software (RX Solutions, Chavanod, France). Image processing was performed with CTAn software (Bruker µCT, France) allowing quantification of pore properties within the analyzed structures. Here, the porosity [%] is the void fraction within the volume of sample analyzed after an automatic threshold based on Otsu method. The size of the pores was derived from the local thickness calculation (i.e. the diameter of the largest sphere which encloses a point in the void and which is entirely bounded within the solid surfaces) as well as the size of the walls (Hildebrand & Rüegsegger, 1997). Samples of doughs and breads were analyzed in triplicates and samples of partial baking in duplicates.

2.5. Statistical analysis

The statistical analysis was performed using Statgraphics Centurion 19 (Statpoint Technologies, Virginia, USA). A one-way ANOVA ($p < 0.05$) and Fisher's least significant difference (LSD) multiple sample comparison procedure was selected to assess significant differences among the samples. Pearson correlation test ($p < 0.05$) was applied to analyze correlations between parameters. If not indicated otherwise, results are reported as mean values ± standard deviation.

3. Results & discussion

3.1. Void fraction and electrical conductivity of model bread doughs

The aim of this study was to produce model bread doughs with varying initial DVF, primarily controlled by proofing time, and initial EC, influenced by both salt addition and proofing time. The results are demonstrated in Table 1. For clarity and comprehensibility, the six model doughs have been designated A to F and are retained in the same order in the following sections, except for the designation of the standard deviation.

DVF were found to be in the range of 16–20 % for doughs without proofing step, consistent with results from Jha et al. (2017), and up to 65–69 % for 90 min of proofing as also reported by Raad et al. (2025). The DVF in dough after proofing depends strongly on yeast activity. Longer proofing times result in higher DVF (Zúñiga & Le-Bail, 2009), as also found in the results of this study. Also initial DVF plays a role as higher DVF are connected to a larger interfacial area for mass transfer of produced CO_2 during proofing (Jha et al., 2017). Additionally, yeast productivity is affected by external factors like temperature and recipe components such as salt which is known to reduce fermentative performance by decreasing cell viability (Struyf et al., 2017). This effect was reflected in the reduced DVF of doughs with 1.5 % salt compared to those with 0.5 % salt after 0–45 min of proofing (Table 1), consistent with results obtained by Shehzad et al. (2010). Simultaneously, salt

addition seemed to enhance gas retention, leading to greater DVF in doughs with 1.5 % salt after 90 min of proofing. This finding confirms previous studies (Beck et al., 2012a, 2012b; Lynch et al., 2009) that demonstrated that differences in DVF were associated with strengthening of the gluten network while rheological properties remained unaffected. The EC of the dough was both influenced by the addition of salt and the DVF in the dough, confirmed by performing a simplified correlation test (see Table A1 in supplementary material Appendix A). Higher DVF led to reduced EC as gas cells are poor electrical conductors and limit the availability for current to flow (Waldert et al., 2025b), whereas salt addition increased EC caused by higher concentration of ionic compounds.

To clarify the impact of salt on EC, two concurrent mechanisms need to be considered: (i) salt inhibits fermentation, reducing DVF and thereby diminishing the insulating effect of air for current flow during ohmic baking; and (ii) salt directly raises the ionic concentration and EC of the liquid, current-transmitting dough phase. In the presented results (Table 1), the first mechanism is more evident at early proofing (0–45 min), where lower DVF coincide with higher EC in the doughs with 1.5 % salt, whereas the second mechanism is consistently present across all times. At late proofing (90 min), enhanced gas retention can increase DVF even in high-salt doughs, partially offsetting the ionic gain. Together, these trends explain why EC can be statistically comparable for doughs with opposite extremes of salt and proofing time for dough A featuring the two extremes of low salt content and 0 min proofing time as well as dough F with high salt content and 90 min proofing time. Additionally, changes in EC depending on the DVF (d(EC)/d(DVF)) were more pronounced for doughs D-F featuring the higher initial salt content, as visualized in Figure A1 in supplementary material Appendix A. The effect of predefined dough properties on process progression and structure development is evaluated in the next sections.

3.2. Ohmic baking process characterization

The characterization of the ohmic baking process included temperature and current intensity measurements. The progression of core temperature is shown in Fig. 2. The doughs followed an almost linear heating profile up to 80 °C, as defined by the PID-controlled linear temperature ramp, in agreement with previous findings on ohmic baking of wheat bread (Gally et al., 2016; Kulishov et al., 2020; Waldert et al., 2025b). Overall, maximum differences in temperature were limited to 10 °C, and all doughs exceeded the starch gelatinization threshold of around 68 °C (Li et al., 2004) after the heating phase of 12 min. Overall, heating rates were in a positive relation with EC and the average across all trials was 6.4 ± 0.3 °C/min. Doughs D-F with ECs in the range of 1.0–2.4 mS/cm (containing 1.5 % salt) exhibited a stable heating curve, reaching 98 °C within the target of 12 min while those below 1.0 mS/cm showed slightly slower heating behavior. In the "worst-case" scenario, highest DVF combined with lowest EC (dough C), the applied energy was insufficient to offset heat losses to the surroundings at $T > 80$ °C as the dough did not reach 98 °C within the defined treatment duration. This effect results from the voltage-based temperature control and limited operating range of the PID controller, which could not deliver enough energy due to the dough's higher electrical resistance. It highlights the critical role of EC in determining heating behavior and energy conversion efficiency during ohmic baking (Jaeger et al., 2016). Fig. 3 visualizes these interdependencies by plotting the progression of current intensity of each model dough over temperature increase during the treatment. Across all doughs, current intensity rose slightly up until ~40 °C, remained nearly constant to ~90 °C, and decreased slightly towards the end of baking.

Under constant applied voltage and fixed electrode spacing, this trajectory reflects two concurrent influences. The first influencing factor covers geometric changes, as the effective current cross-section increases during dough volume expansion, which tend to raise current intensity for a given EC. Secondly, raw material changes play a role that make the EC evolution dynamic, including temperature-dependent ion mobility (early rise), starch gelatinization and protein denaturation that reduce continuous liquid pathways (mid-stage plateau and further decline), and progressive water evaporation (late-stage decline). The

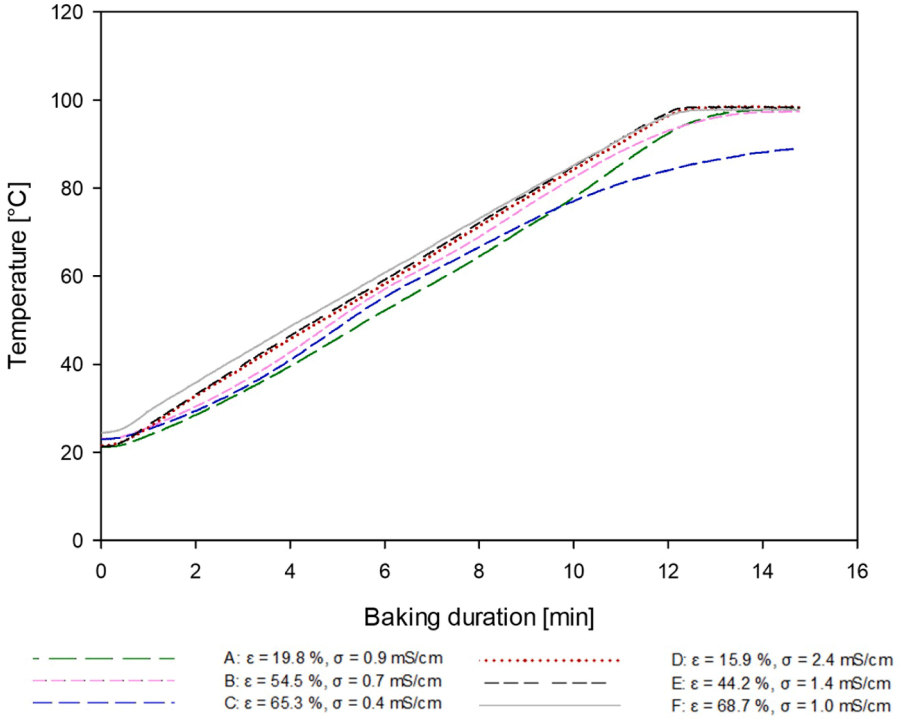

Fig. 2. Average temperature progression (geometrical centre) in wheat model doughs A-F during ohmic baking ($n = 3$), depending on the initial void fraction (ε) and electrical conductivity (σ). Salt content was 0.5 % (w/w flour) for doughs A-C and 1.5 % (w/w flour) for doughs D-F. Proofing time was 0 min for doughs A and D, 45 min for doughs B and E, and 90 min for doughs C and F, respectively. The standard deviation (<1.5 K in all cases) was not added for improved visualisation.

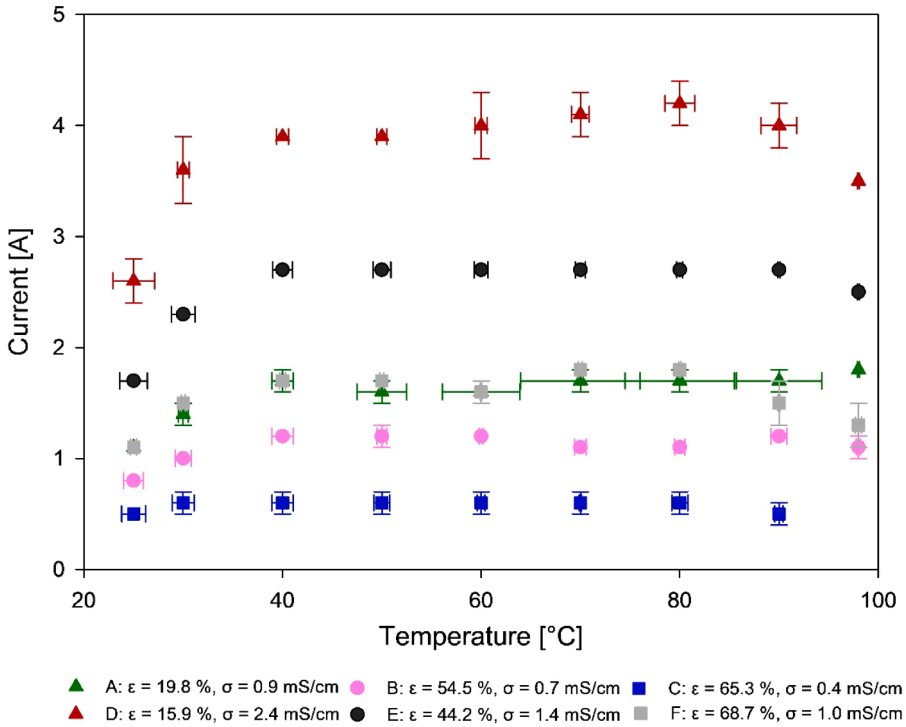

Fig. 3. Progression of current intensity over core temperature (geometrical centre) in wheat model doughs A-F during ohmic baking ($n = 3$). Values are ranging from 25 °C (initial dough temperature) to 98 °C (holding temperature, if reached), depending on the initial void fraction (ε) and electrical conductivity (σ). Salt content was 0.5 % (w/w flour) for doughs A-C and 1.5 % (w/w flour) for doughs D-F. Proofing time was 0 min for doughs A and D, 45 min for doughs B and E, and 90 min for doughs C and F, respectively.

resulting effect is that the EC of bread largely mirrors the values of dough, even in high-porosity, lower-moisture breads, with slight decreases (Table 1). Similar trends have been reported in previous studies, though with a more pronounced EC decline in the final stages of baking, attributed to the expanding current cross-sectional area and reduced water availability from evaporation and starch–protein interactions (Kulishov et al., 2020; Waldert et al., 2025b). Importantly, beyond the well-known principle that higher initial EC accelerates early heating, the dynamic progression pattern during ohmic baking provides deeper process insights. A fuller resolution of these stages would be needed as guidance for future industrial implementation but requires real-time impedance monitoring to separate matrix mobility from porosity and network effects, which may also differ across generator types and their current-control strategies, limiting the extent of comparison.

Doughs A-C featuring EC < 1.0 mS/cm (0.5 % salt) exhibited lower current flow due to reduced concentration of ionic compounds compared to 1.5 % salt formulations in doughs D-F. Within a given salt concentration, current flow decreased with higher DVF due to more non-conductive gas cells and increased proportionally to the dough mass (visualized in Figure A1, supplementary material Appendix A) in similar ratios (r) to the salt concentration ($r = 3$), specifically $r_{600} = 2.5$ (600 g), $r_{450} = 2.0$ (450 g), and $r_{300} = 2.5$ (300 g), respectively. Similar results were observed by Gally et al. (2016) for dough DVF ranging from 10.8 - 60.1 %. Interestingly, the doughs A and F displayed similar current flows, reflecting their comparable EC values (Table 1). Despite this, their heating behavior differed between 25–80 °C (Fig. 2). This difference can be explained by dough mass (600 g for dough A vs. 300 g for dough F, see Figure A1, supplementary material Appendix A) and the ohmic generator's operating principle, which adjusted current intensity and pulse output according to the predefined temperature-time profile. At higher EC in the current transmitting dough matrix (> 1.0 mS/cm), each pulse delivered more energy (0.5–0.8 kW/kg) compared to lower EC (0.2–0.5 kW/kg). Combined with lower dough masses, this resulted in higher power consumption (see Table 1) and slightly faster heating. Importantly, accumulated power consumption, relevant for industrial application and process efficiency, rose significantly only in doughs with both high EC and high DVF, reflecting the interplay of increased EC in the dough matrix, its mass, and resistance from different amounts of non-conductive gas cells. Generally, energy consumption could be reduced drastically compared to conventional bread baking with ~4 MJ/kg (Le-Bail et al., 2010) when using ohmic baking (~0.3 MJ/kg).

In ohmically baked breads (see Table 1), porosity ranged from 66 % to 82 % and was no longer influenced by initial EC but depended solely on the initial DVF. Jha et al. (2017) measured a porosity of 83 % for conventionally baked sandwich breads prepared from doughs under similar conditions as done in the current study which demonstrates that ohmic baking can result in similar porosities compared to conventional baking. This highlights the importance of gas cell expansion during ohmic baking of yeast-leavened wheat doughs which evens out differences in the dough properties if performed under comparable and optimized conditions. However, as parameters like texture or pore structure might have been affected by the dough properties, the following sections shed light on physical bread properties and microstructural development during ohmic baking.

3.3. Physical bread properties

Exemplary pictures of cross-sections of ohmically baked breads are shown in Fig. 4. The objective difference between doughs with initial DVF ranging from 15–55 % (Fig. 4A-B and D-E) appeared only minor whereas larger pore sizes were clearly noticeable when the DVF exceeded 65 % (Fig. 4C and F), independently of the initial EC. The corresponding quantified physical bread properties are listed in Table 2. With increasing DVF, the crumb structure revealed larger, more inhomogeneous pores and a lower total amount. Crumb hardness was decreasing with increasing DVF and decreasing EC. Baking loss and crumb elasticity remained mostly unaffected while the specific volume increased. All these effects seemed mostly unaffected by initial EC.

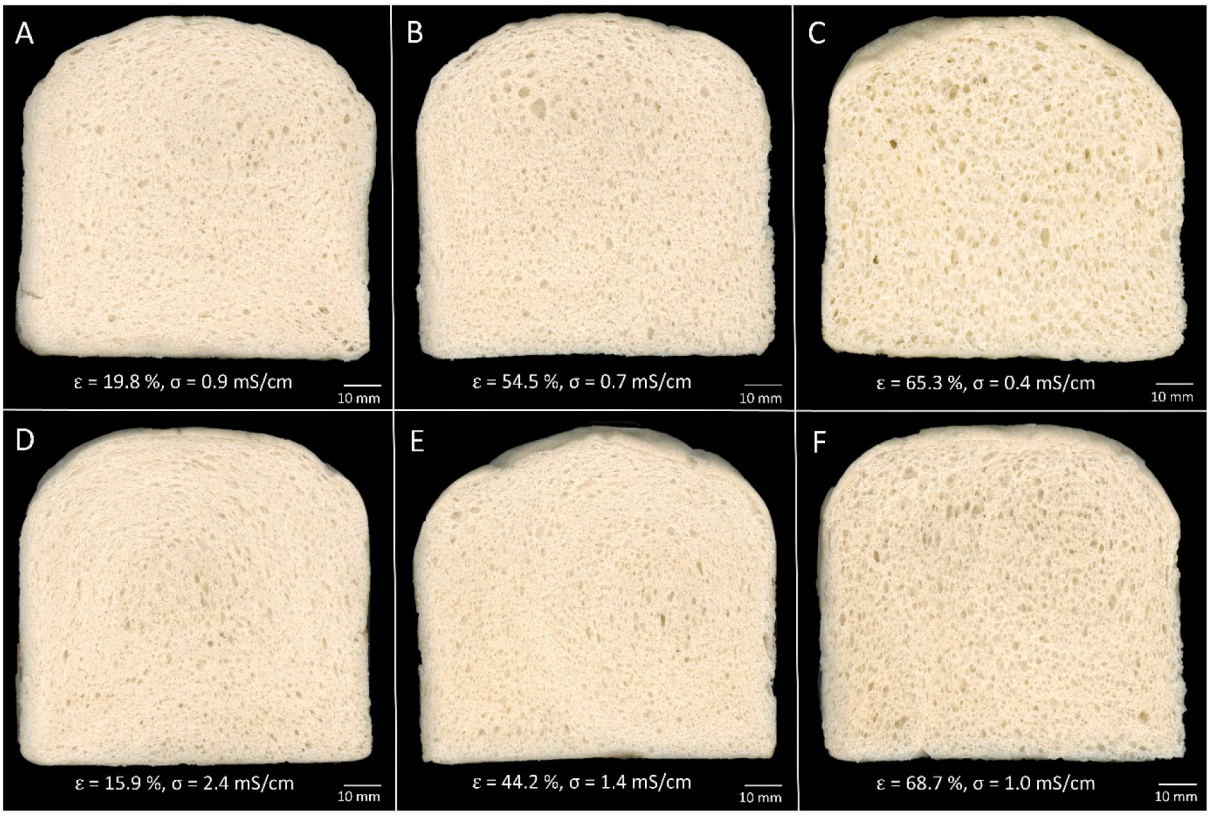

Fig. 4. Cross-sections of ohmically baked breads (not to scale) with either 0.5 % salt (w/w flour) for slices A-C or 1.5 % salt (w/w flour) for slices D-F. Different proofing times were realized before baking: 0 min (A, D), 45 min (B,E) and 90 min (C,F). Resulting initial void fractions (ε) and electrical conductivities (σ) of the corresponding bread doughs are noted.

Table 2
Physical bread properties after ohmic baking, depending on the initial void fraction (ε) and electrical conductivity (σ) of the dough.

Model doughs*			Resulting physical bread properties						
	ε_{Dough} [%]	σ_{Dough} [mS/cm]	Baking loss [%]	Specific volume [ml/g]	Crumb hardness [N]	Crumb elasticity [%]	Pore count [-]	Pore size [mm^2]	Pore inhomogeneity [mm^2]
A	**19.8**	**0.9**	5.9 ± 0.6^{A}	2.12 ± 0.09^{A}	9.5 ± 2.7^{C}	56.3 ± 1.9^{B}	1980 ± 159^{C}	0.05 ± 0.01^{A}	0.26 ± 0.05^{AB}
B	**54.5**	**0.7**	7.4 ± 1.1^{ABC}	2.87 ± 0.18^{C}	4.9 ± 1.0^{B}	55.9 ± 1.3^{B}	1664 ± 139^{B}	0.07 ± 0.01^{C}	0.28 ± 0.06^{B}
C	**65.3**	**0.4**	8.6 ± 1.3^{C}	3.37 ± 0.07^{D}	2.8 ± 0.3^{A}	45.1 ± 4.7^{A}	1149 ± 173^{A}	0.11 ± 0.02^{E}	0.48 ± 0.08^{D}
D	**15.9**	**2.4**	5.8 ± 0.1^{A}	1.95 ± 0.15^{A}	13.4 ± 2.9^{D}	53.5 ± 2.7^{AB}	2126 ± 191^{D}	0.05 ± 0.01^{A}	0.22 ± 0.05^{A}
E	**44.2**	**1.4**	6.8 ± 0.6^{AB}	2.56 ± 0.08^{B}	8.2 ± 1.3^{C}	52.9 ± 2.0^{B}	1767 ± 80^{B}	0.06 ± 0.01^{B}	0.25 ± 0.02^{AB}
F	**68.7**	**1.0**	8.2 ± 1.5^{BC}	3.42 ± 0.04^{D}	3.6 ± 0.3^{AB}	52.9 ± 3.8^{AB}	1236 ± 123^{A}	0.10 ± 0.01^{D}	0.41 ± 0.07^{C}

Technical replicates ($n = 3$ for baking loss and specific volume, $n = 9$ for crumb and pore parameters) were performed. Significant differences ($p < 0.05$) are depicted as different capital letters within one data column.

* Salt content was 0.5 % (w/ w flour) for doughs A-C and 1.5 % (w/ w flour) for doughs D-F. Proofing time was 0 min for doughs A and D, 45 min for doughs B and E, and 90 min for doughs C and F, respectively.

To understand correlations between the parameters of interest, DVF and EC, with selected bread properties, a correlation test was performed (Table 3) which reveals strong negative (−1) or positive correlations (+1), respectively. The results confirm that the initial DVF significantly influenced almost all physical bread properties, especially strong for specific volume, crumb hardness as well as pore count and pore size, in alignment with previous findings conducted for conventional oven baking (Jha et al., 2017; Raad et al., 2025). Interestingly, EC influenced only the crumb hardness. This translates into the fact that initial dough formulation in terms of different EC did not affect the final bread properties in alignment with the observation in Table 1 that EC did not change much from dough to bread (as explained in Section 3.2). Here, it needs to be mentioned that EC is temperature dependent and was not estimated at the same temperature for dough (20 °C) and bread (98 °C), so the EC of breads is supposedly slightly lower when measured at 20 °C. In any case, the sensitivity of EC changes in porosity (d(EC)/d(porosity) was markedly greater in breads than in doughs, as presented in Figure A2 in supplementary material Appendix A. Opposite to that, initial DVF significantly impacted final bread characteristics as also the bread porosity was affected by it (Table 1). Moreover, crumb texture properties correlated with pore structure and specific volume was partially influenced by the crumb properties including pore structure

Table 3
Simplified correlations between initial void fraction (ε) and electrical conductivity (σ) in wheat dough and resulting physical bread properties after ohmic baking. Significant values ($p < 0.05$) are marked with *.

	ε_{Dough} [%]	σ_{Dough} [mS/cm]	Baking loss [%]	Specific volume [ml/g]	Crumb hardness [N]	Crumb elasticity [%]	Pore count [-]	Pore size [mm^2]
Baking loss [%]	0.50*	−0.21						
Specific volume [ml/g]	0.76*	−0.36	0.75*					
Crumb hardness [N]	−0.92*	0.87*	−0.36	−0.62*				
Crumb elasticity [%]	−0.57*	0.27	−0.31	−0.58*	0.50*			
Pore count [-]	−0.92*	0.65*	−0.51*	−0.67*	0.87*	0.66*		
Pore size [mm^2]	0.89*	−0.61*	0.56*	0.76*	−0.85*	−0.74*	−0.97*	
Pore inhomogeneity [mm^2]	0.26	−0.31	0.08	0.09	−0.28	0.37	−0.08	−0.04

and texture.

The findings align with other studies (Beck et al., 2012b; Lynch et al., 2009) which demonstrated no significant influence of the initial salt content on baking loss, crumb hardness or pore properties but higher specific volumes for conventionally baked breads with lower salt addition. However, previous studies have only analyzed breads after 60–90 min of proofing whereas the current study reveals differences in case of lower proofing times. For pore inhomogeneity, salt only enhanced uniformity of crumb structure after 90 min of proofing, consistent with results by Lynch et al. (2009). Higher initial DVF in the dough also revealed a softer bread crumb after conventional baking in the study of Lampignano et al. (2013) where the reason could be connected to a lower quantity of pores connected with higher pore diameters as a higher number of smaller pores resulted in a harder crumb texture. As many mechanical bread properties are related to its microstructure (Falcone et al., 2004; Jekle & Becker, 2015), this topic is covered in detail in the next section.

3.4. Analysis of microstructural changes during ohmic baking

This section characterizes the evolution of 3D microstructure obtained from XMT in raw doughs A-F with different initial DVF and EC and their corresponding breads as well as intermediate baking stages at 48 °C, 68 °C and 98 °C (Fig. 5). Although 2D analysis of macroscopic structures is common and requires minimal sample preparation, 3D imaging provides more precise information on cell shape, distribution, wall thickness, pore openness, and structural evolution during processing (Le-Bail et al., 2009; Wang et al., 2011). For a comprehensive visualization, Fig. 6 presents the progression of porosity, pore size (diameter), and wall thickness during ohmic baking. Detailed numerical values and statistical outputs are provided in Table A2 of supplementary material Appendix A.

When comparing results from porosity measurements in Table 1 with the values obtained from XMT analysis for doughs and breads, the trends appear comparable, but XMT results are generally lower. This difference might arise from the sample preparation with the freezing step, the subsampling of a volume inside the sample, even though preliminary studies on bread helped to define the representative sample volumes, or the thresholding method that might overestimate the walls because of grey levels in images due to partial volume effect. Generally, the microstructural evolution during proofing and baking followed a clear trajectory in which average pore size (Fig. 6i) and overall porosity (Figure 6iii) followed a similar increasing trend. Pore size was smaller in doughs with EC > 1 mS/cm, likely due to ionic effects on yeast activity (Shehzad et al., 2010), particularly in combination with high DVF. Doughs with DVF > 65 % consistently exhibited larger pores and higher porosity throughout baking and in the final bread, with the largest pores occurring in breads with high DVF but low EC. This observation confirms the results for pore size obtained from 2D analysis of bread slices in Table 2. Also Lampignano et al. (2013) noted greater heterogeneity in pore size and shape in conventionally baked breads with higher initial DVF. In contrast, smaller and more homogeneous pores were consistently associated with lower DVF, as also mentioned by Jha et al. (2017). After kneading, dough usually exhibits a homogeneous distribution of small gas cells. With extended proofing, higher DVF led to larger pores and fewer overall number of cells. Cell expansion and coalescence through gas cell interactions produce increasingly heterogeneous structures with irregular, non-spherical cavities, especially at DVF above 50 % (Babin et al., 2006; Le-Bail et al., 2009; Wang et al., 2011). Moreover, larger gas cells lead to thinner walls, increasing the possibility of cell wall rupture and disconnected lattices in the bread crumb. Lower DVF doughs, however, display a pore network characterized by smaller, more numerous pores (Lampignano et al., 2013).

Pore structure appeared to stabilize at ~68 °C, corresponding to starch gelatinization and protein denaturation as key processes for dough mechanics and gas retention capacity (Jekle & Becker, 2015). The sharp decline and variability in porosity and pore size at 48 °C partial baking reinforces ~68 °C as the critical temperature for structure fixation. At this stage, the dough matrix could not maintain pore stability during cooling, an effect likely amplified in ohmically baked breads due to the lack of crust formation. This collapse was less pronounced in low-DVF doughs. For better visualization, exemplary pictures of breads are added in Table A3 and Table A4 in supplementary material Appendix A. While breads with higher initial DVF maintained greater porosity, these differences diminished in the final product due to structural collapse during cooling. This indicates that high DVF promoted pore expansion but reduced structural fixation, whereas low DVF favored matrix stabilization. Physical characterization confirmed that breads from low-DVF doughs exhibited a higher number of smaller pores, which improved structural retention, as also visible in partially baked samples at 98 °C (Figure 6ii). Similar observations were reported by Shehzad et al. (2010), who linked larger gas bubbles at the microscale to reduced stability at the macroscale.

Wall thickness (Fig. 6i), representing the solid matrix surrounding gas cells through which current is transmitted, remained largely constant during baking, except for collapse effects observed at 48 °C. Final breads exhibited comparable wall thickness values, which appeared to eventually stabilize at ~68 °C in low-DVF doughs and ~98 °C in high-DVF doughs. The numerical values are consistent with reported values of 0.34–0.46 mm for conventionally baked wheat bread (Bellido et al., 2006). During conventional baking, volume usually increases until ~50 °C, followed by a decrease and subsequent stabilization above 75 °C. At this stage, porosity stabilizes at 70–80 %, reflecting the transition from dough to crumb through starch gelatinization, protein denaturation, and gluten cross-linking. The distribution of gas cells and cell wall thickness remains largely consistent with structures formed during proofing (Babin et al., 2006). Opposite to that, ohmic baking volume increase is most pronounced in temperatures over 50 °C and consistent in rising until reaching 100 °C (Waldert et al., 2025b). Although this study did not explicitly address the mechanisms of structure creation and fixation in ohmic baking compared to conventional baking, these aspects represent a logical direction for future work. Moreover, the quantification of open and closed cells would give further insight into relation to microstructural changes and macroscopic stability. For conventionally

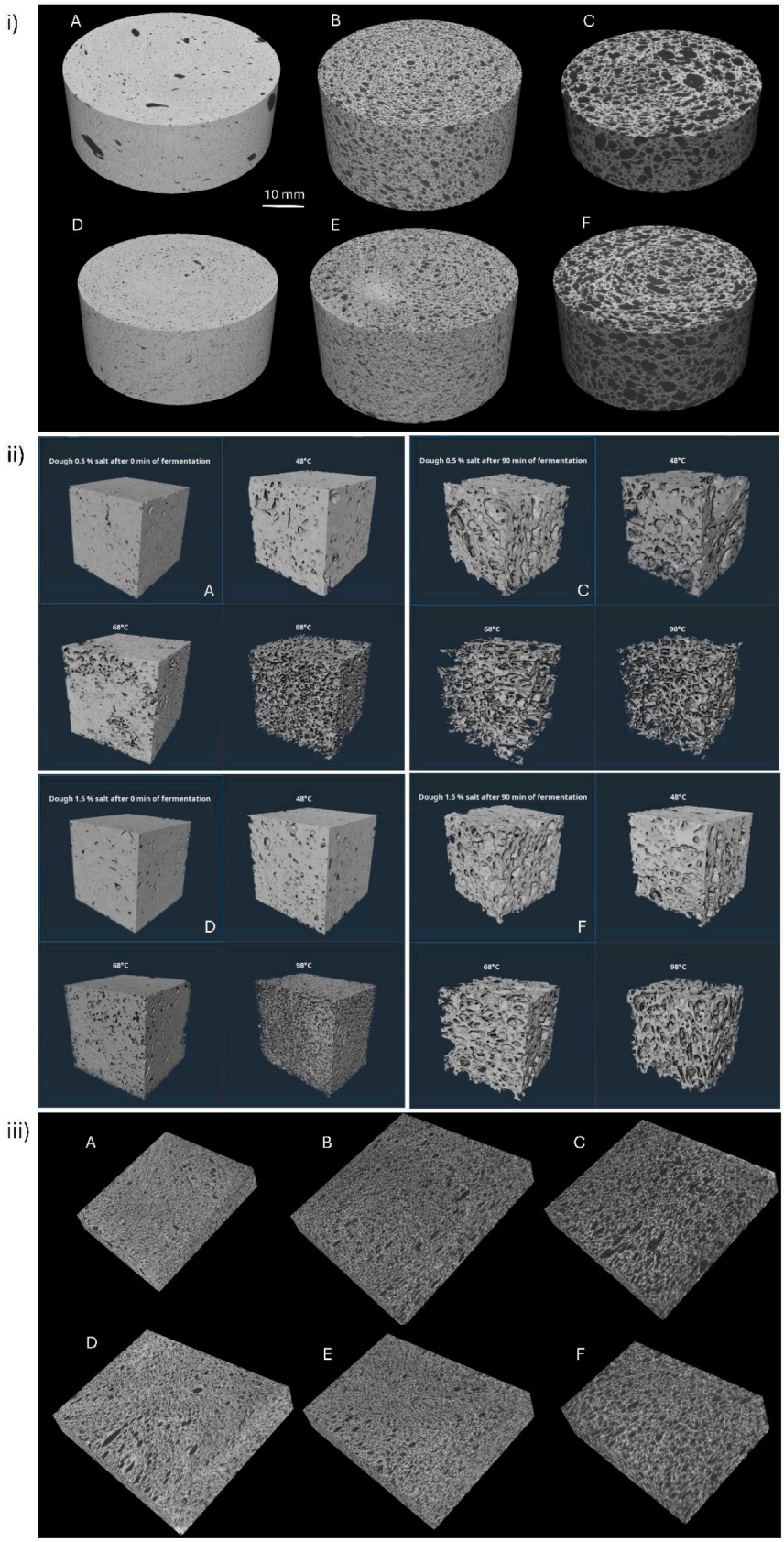

Fig. 5. 3D-representations of i) bread doughs A-F after proofing, ii) resulting partially baked samples for doughs A, C, D and F (1 cm^3, 200 × 200 × 200 voxels of 50 μm), and iii) resulting bread slices (not to scale). Dough recipes contained either 0.5 % salt (w/w flour) for doughs A-C or 1.5 % salt (w/w flour) for doughs D-F, including different proofing times of 0 min (A, D), 45 min (B, E) and 90 min (C, F).

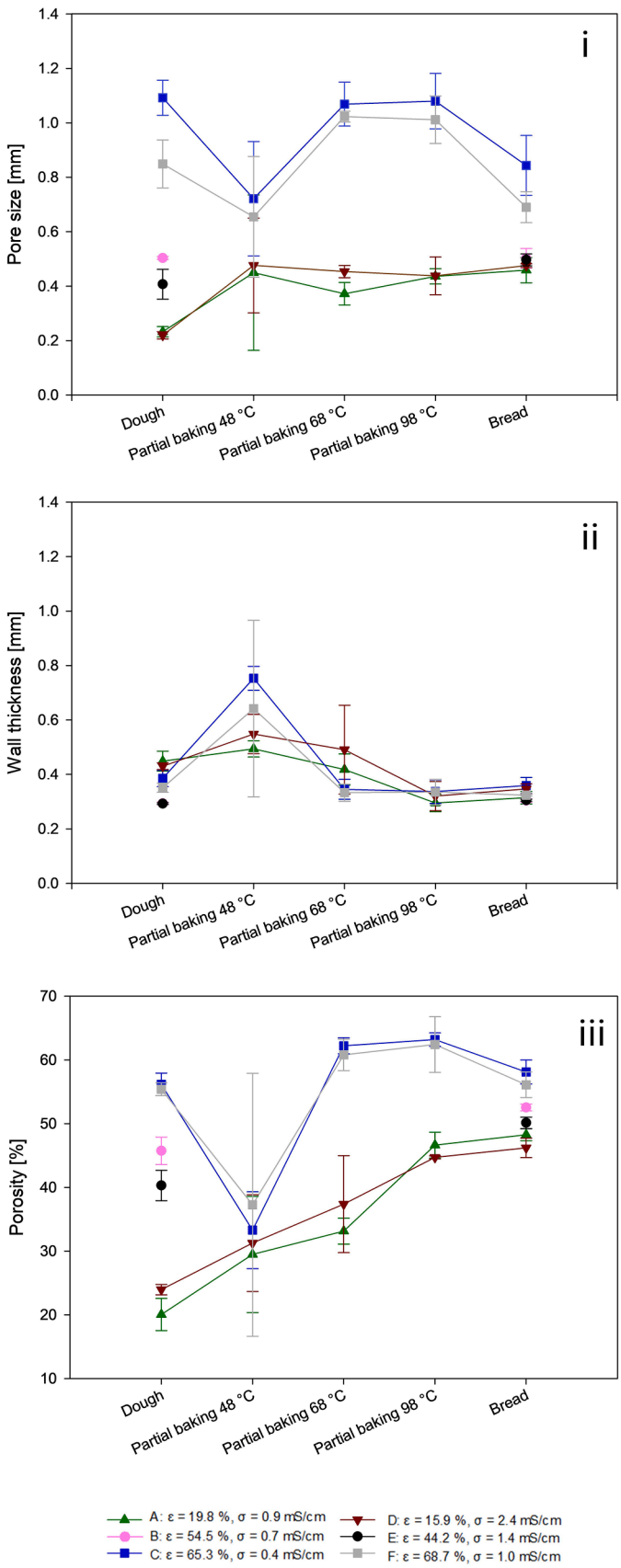

(caption on next column)

Fig. 6. Progression of average pore size (i), wall thickness (ii) and porosity (iii) obtained from 3D-image analysis of raw doughs A-F, partially baked doughs and final breads in dependency of the initial void fractions (ε) and electrical conductivity (σ). Results for dough and bread are displayed as mean values ($n = 3$) and standard deviation. Partially baked dough samples (not applicable for doughs B and E) are displayed as mean values ($n = 2$) and span width. Salt content was 0.5 % (w/w flour) for doughs A-C and 1.5 % (w/w flour) for doughs D-F. Proofing time was 0 min for doughs A and D, 45 min for doughs B and E, and 90 min for doughs C and F, respectively.

baked breads, the open cell is usually one single gas cell making up 99 % of the total porosity. An increase in the number of pores therefore means the creation of closed cells which further affect friability of breads (Wang et al., 2011). It would be interesting to see if this effect is also applicable for ohmically baked breads.

4. Conclusions

This study advances understanding of the micro- and macroscale structural development of ohmically baked wheat bread and clarifies the interactions among dough properties, baking conditions, and final product quality. EC was the dominant factor governing heating behavior, as current conduction occurs only in the solid dough phase. Baking at EC values above 1 mS/cm improved current flow and temperature control, supporting the use of in-line conductivity monitoring with power modulation for active process control and modeling. DVF primarily influenced process–structure relationships, strongly correlating with bread volume and crumb texture. Although overall porosity was similar, higher DVF led to larger pores, while lower DVF produced smaller, more uniform pores, resulting in lower volume and firmer crumb. X-ray microtomography proved valuable for non-destructive 3D characterization, identifying a critical structure-fixation temperature around 68 °C. Overall, targeted adjustment of DVF and EC enables the tailored control of ohmic baking outcomes, supporting both product quality and process sustainability, while offering a foundation for future studies on localized structural dynamics. Future research should also incorporate sensory analysis into the product quality assessment to evaluate the flavor and palatability of breads with different DVF and EC as valuable guidance for industrial implementation.

Funding sources

This research did not receive any specific grant from funding agencies in the public, commercial, or not-for-profit sectors.

Declaration of generative AI and AI-assisted technologies in the manuscript preparation process

During the preparation of this work the author(s) used ChatGPT in order to improve stylistic elements of the text. After using this tool/service, the author(s) reviewed and edited the content as needed and take(s) full responsibility for the content of the published article.

Ethical statement - studies in humans and animals

The authors declare that this study did not involve Humans or Animals.

CRediT authorship contribution statement

Kate Waldert: Writing – original draft, Visualization, Validation, Methodology, Investigation, Formal analysis, Conceptualization. **Sylvie Swyngedau Chevallier:** Writing – review & editing, Visualization, Validation, Methodology, Investigation, Formal analysis. **Olivier Rouaud:** Writing – review & editing, Supervision, Project administration, Conceptualization. **Alain Le-Bail:** Writing – review & editing,

Supervision, Resources, Conceptualization. **Henry Jäger:** Writing – review & editing, Supervision, Conceptualization.

Declaration of competing interest

The authors declare that they have no known competing financial interests or personal relationships that could have appeared to influence the work reported in this paper.

Acknowledgements

The authors would like to thank Christy Raad and Anthony Ogé for their support. Open access funding provided by BOKU University.

Supplementary materials

Supplementary material associated with this article can be found, in the online version, at doi:10.1016/j.afres.2026.101824.

Data availability

Data will be made available on request.

References

Astráin-Redín, L., Waldert, K., Giancaterino, M., Cebrián, G., Álvarez-Lanzarote, I., & Jaeger, H. (2024). Ohmic cooking of carrots: Limitations in the use of power input and cooking value for process characterization. *Journal of Food Engineering, 370*, Article 111974. https://doi.org/10.1016/j.jfoodeng.2024.111974

Babin, P., Della Valle, G. G., Chiron, H., Cloetens, P., Hoszowska, J., Pernot, P., Réguerre, A. L., Salvo, L., & Dendievel, R. (2006). Fast X-ray tomography analysis of bubble growth and foam setting during breadmaking. *Journal of Cereal Science, 43* (3), 393–397. https://doi.org/10.1016/j.jcs.2005.12.002

Beck, M., Jekle, M., & Becker, T. (2012a). Impact of sodium chloride on wheat flour dough for yeast-leavened products. I. Rheological attributes. *Journal of the Science of Food and Agriculture, 92*(3), 585–592. https://doi.org/10.1002/jsfa.4612

Beck, M., Jekle, M., & Becker, T. (2012b). Impact of sodium chloride on wheat flour dough for yeast-leavened products. Ii. Baking quality parameters and their relationship. *Journal of the Science of Food and Agriculture, 92*(2), 299–306. https://doi.org/10.1002/jsfa.4575

Bellido, G. G., Scanlon, M. G., Page, J. H., & Hallgrimsson, B. (2006). The bubble size distribution in wheat flour dough. *Food Research International, 39*(10), 1058–1066. https://doi.org/10.1016/j.foodres.2006.07.020

Bender, D., Gratz, M., Vogt, S., Fauster, T., Wicki, B., Pichler, S., Kinner, M., Jäger, H., & Schoenlechner, R. (2019). Ohmic heating–A novel approach for gluten-free bread baking. *Food and Bioprocess Technology, 12*(9), 1603–1613. https://doi.org/10.1007/s11947-019-02324-9

Chevallier, S., Réguerre, A.-L., Le Bail, A., & Della Valle, G. G. (2014). Determining the cellular structure of two cereal food foams by X-ray micro-tomography. *Food Biophysics, 9*, 219–228. https://doi.org/10.1007/s11483-014-9336-5. Advance online publication.

Datta, A. K., Sahin, S., Sumnu, G., & Ozge Keskin, S. (2007). Porous media characterization of breads baked using novel heating modes. *Journal of Food Engineering, 79*(1), 106–116. https://doi.org/10.1016/j.jfoodeng.2006.01.046

Derde, L. J., Gomand, S. V., Courtin, C. M., & Delcour, J. A. (2014). Moisture Distribution during Conventional or Electrical Resistance Oven Baking of Bread Dough and Subsequent Storage. *Journal of agricultural and food chemistry, 62*(27), 6445–6453. https://doi.org/10.1021/jf501856s

Falcone, P. M., Baiano, A., Zanini, F., Mancini, L., Tromba, G., Montanari, F., & Del Nobile, M. A. (2004). A novel approach to the study of bread porous structure: Phase-Contrast X-ray microtomography. *Journal of Food Science, 69*(1). https://doi.org/10.1111/j.1365-2621.2004.tb17865.x

Gally, T., Rouaud, O., Jury, V., Havet, M., Ogé, A., & Le-Bail, A. A. (2017). Proofing of bread dough assisted by ohmic heating. *Innovative Food Science & Emerging Technologies, 39*, 55–62. https://doi.org/10.1016/j.ifset.2016.11.008

Gally, T., Rouaud, O., Jury, V., & Le-Bail, A. A. (2016). Bread baking using ohmic heating technology; a comprehensive study based on experiments and modelling. *Journal of Food Engineering, 190*, 176–184. https://doi.org/10.1016/j.jfoodeng.2016.06.029

Giancaterino, M., Waldert, K., Prenner, S. E., Mair, D., & Jäger, H. (2025). Synergistic effects of pulsed electric fields and ohmic heating on red beetroot cooking performance. *Innovative Food Science & Emerging Technologies, 104*, Article 104089. https://doi.org/10.1016/j.ifset.2025.104089

He, H., & Hoseney, R. C. (1991). A critical look at the electric resistance oven. *Cereal chemistry, 68*(2), 151–155.

Hildebrand, T., & Rüegsegger, P. (1997). A new method for the model-independent assessment of thickness in three-dimensional images. *Journal of Microscopy, 185*(1), 67–75. https://doi.org/10.1046/j.1365-2818.1997.1340694.x

Jaeger, H., Roth, A., Toepfl, S., Holzhauser, T., Engel, K.-. H., Knorr, D., Vogel, R. F., Bandick, N., Kulling, S., Heinz, V., & Steinberg, P. (2016). Opinion on the use of ohmic heating for the treatment of foods. *Trends in Food Science & Technology, 55*, 84–97. https://doi.org/10.1016/j.tifs.2016.07.007

Jekle, M., & Becker, T. (2015). Wheat dough microstructure: The relation between visual structure and mechanical behavior. *Critical Reviews in Food Science and Nutrition, 55* (3), 369–382. https://doi.org/10.1080/10408398.2012.656476

Jha, P. K., Chevallier, S., Cheio, J. J., Rawson, A., & Le-Bail, A. A. (2017). Impact of resting time between mixing and shaping on the dough porosity and final cell distribution in sandwich bread. *Journal of Food Engineering, 194*, 15–23. https://doi.org/10.1016/j.jfoodeng.2016.07.016

Khatir, Z., Paton, J., Thompson, H., Kapur, N., & Toropov, V. (2013). Optimisation of the energy efficiency of bread-baking ovens using a combined experimental and computational approach. *Ap. Energy, 112*, 918–927. https://doi.org/10.1016/j.apenergy.2013.02.034

Kulishov, B., Kulishova, K., Rudometova, N., Fedorov, A., & Novoselov, A. (2020). Advantages of electric resistance method for baking bread and flour confectionery products of functional purpose. *Agronomy Research*, (18), Article 4. https://doi.org/10.15159/AR.20.211 (774.0Kb.

Lampignano, V., Laverse, J., Mastromatteo, M., & Del Nobile, M. A. (2013). Microstructure, textural and sensorial properties of durum wheat bread as affected by yeast content. *Food Research International, 50*(1), 369–376. https://doi.org/10.1016/j.foodres.2012.10.030

Le-Bail, A. A., Boumali, K., Jury, V., Ben-Aissa, F., & Zuniga, R. (2009). Impact of the baking kinetics on staling rate and mechanical properties of bread crumb and degassed bread crumb. *Journal of Cereal Science, 50*(2), 235–240. https://doi.org/10.1016/j.jcs.2009.05.008

Le-Bail, A. A., Dessev, T., Jury, V., Zuniga, R., Park, T., & Pitroff, M. (2010). Energy demand for selected bread making processes: Conventional versus part baked frozen technologies. *Journal of food engineering, 96*(4), 510–519. https://doi.org/10.1016/j.jfoodeng.2009.08.039

Li, F.-D., Li, L.-T., Li, Z., & Tatsumi, E. (2004). Determination of starch gelatinization temperature by ohmic heating. *Journal of Food Engineering, 62*(2), 113–120. https://doi.org/10.1016/S0260-8774(03)00199-7

Lynch, E. J., Dal Bello, F., Sheehan, E. M., Cashman, K. D., & Arendt, E. K. (2009). Fundamental studies on the reduction of salt on dough and bread characteristics. *Food Research International, 42*(7), 885–891. https://doi.org/10.1016/j.foodres.2009.03.014

Masure, H. G., Wouters, A. G. B., Fierens, E., & Delcour, J. A. (2019). Electrical resistance oven baking as a tool to study crumb structure formation in gluten-free bread. *Food research international (Ottawa, Ont.), 116*, 925–931. https://doi.org/10.1016/j.foodres.2018.09.029

Panirani, P. N., Darvishi, H., Hosainpour, A., & Behroozi-Khazaei, N. (2023). Comparative study of different bread baking methods: Combined ohmic – infrared, ohmic – conventional, infrared – conventional, infrared, and conventional heating. *Innovative Food Science and Emerging Technologies, 86*. https://doi.org/10.1016/j.ifset.2023.103349

Pichler, E. C., Schönlechner, R., Różyło, R., Dziki, D., & Świeca, M. (2024). Addition of micronized oat husk fiber to gluten-free bread - Effects on chemical, physical and physiolgical properties. *Journal of Cereal Science, 118*, Article 103981. https://doi.org/10.1016/j.jcs.2024.103981

Raad, C., Le-Bail, P., & Le-Bail, A. A. (2025). Impact of Dough Mixing Pressure with Air and CO2 gases on Dough and Bread properties. *Applied Food Research, 5*(2), Article 101470. https://doi.org/10.1016/j.afres.2025.101470. Advance online publication.

Rumler, R., Bender, D., & Schoenlechner, R. (2023). Mitigating the effect of climate change within the cereal sector: Improving rheological and baking properties of strong gluten wheat doughs by blending with specialty grains. *Plants (Basel, Switzerland), 12*(3). https://doi.org/10.3390/plants12030492

Sadot, M., Cheio, J. J., & Le-Bail, A. A. (2017). Impact on dough aeration of pressure change during mixing. *Journal of Food Engineering, 195*, 150–157. https://doi.org/10.1016/j.jfoodeng.2016.09.008

Shehzad, A., Chiron, H., Della Valle, G. G., Kansou, K., Ndiaye, A., & Réguerre, A. L. (2010). Porosity and stability of bread dough during proofing determined by video image analysis for different compositions and mixing conditions. *Food Research International, 43*(8), 1999–2005. https://doi.org/10.1016/j.foodres.2010.05.019

Struyf, N., van der Maelen, E., Hemdane, S., Verspreet, J., Verstrepen, K. J., & Courtin, C. M. (2017). Bread dough and baker's yeast: An uplifting synergy. *Comprehensive Reviews in Food Science and Food Safety, 16*(5), 850–867. https://doi.org/10.1111/1541-4337.12282

Varayil, H., Loisel, C., Oge, A., Ribette-Lancelot, E., Fontaine, J., Cheio, J. J., Yadav, B. K., & Le-Bail, A. A. (2019). Impact of pressure change during dough mixing and characteristics of bread under high pressure. *International Journal of Pure & Applied Bioscience, 7*(3), 397–404. https://doi.org/10.18782/2320-7051.7556

Waldert, K., Bittermann, S., Martinović, N., Schottroff, F., & Jäger, H. (2025a). Ohmic baking of wheat bread – Effect of process parameters on physico-chemical quality attributes. *Journal of Food Engineering, 392*, Article 112493. https://doi.org/10.1016/j.jfoodeng.2025.112493

Waldert, K., Martinović, N., Bittermann, S., Schottroff, F., & Jäger, H. (2025b). Impact of specific power input and treatment chamber design on product-process-interactions during ohmic baking of wheat bread. *Journal of Food Engineering, 396*, Article 112569. https://doi.org/10.1016/j.jfoodeng.2025.112569

Wang, S., Austin, P., & Bell, S. (2011). It's a maze: The pore structure of bread crumbs. *Journal of Cereal Science, 54*(2), 203–210. https://doi.org/10.1016/j.jcs.2011.05.004

Wang, Z., Huang, J., Ma, S., Wang, X., Sun, B., Wang, F., Li, L., & Bao, Q. (2021). Novel heating technologies to improve fermentation efficiency and quality in wheat

products: A short review. *Grain & Oil Science and Technology, 4*(2), 81–87. https://doi.org/10.1016/j.gaost.2021.01.001

Waziiroh, E., Bender, D., Jäger, H., & Schönlechner, R. (2023). Ohmic baking of gluten-free bread: Role of non-gluten protein on GF bread structure and properties. *International Journal of Food Science & Technology, 58*(2), 595–609. https://doi.org/10.1111/ijfs.16206

& Zúñiga, R., & Le-Bail, A. A. (2009). Assessment of thermal conductivity as a function of porosity in bread dough during proving. *Food and Bioproducts Processing, 87*(1), 17–22. https://doi.org/10.1016/j.fbp.2008.04.002.